Indonesian Journal of Material Research
e-ISSN: 2987-1654
Vol. 4, No. 2, July 2026

Indonesian Journal of MATERIAL RESEARCH

Research Paper

Degeneration in Phosphor-within-Glass Encasers Featuring Disparate Phosphor forms Applied to High-Powered LED

Phan Xuan Le[1], Nguyen Thi Phuong Loan[2*], Phan Thi Minh Man[3]

[1] *Faculty of Electrical Engineering Technology, Industrial University of Ho Chi Minh City, Ho Chi Minh City, 70000, Vietnam*
[2] *Faculty of Fundamental 2, Posts and Telecommunications Institute of Technology, Ho Chi Minh City, 70000, Vietnam*
[3] *Faculty of Electrical and Electronics Engineering, Ton Duc Thang University, Ho Chi Minh City, 70000, Vietnam*
[*] **Corresponding author**: ntploan@ptithcm.edu.vn

Abstract

For supplanting traditional illuminating diode units (LED) made of silicone, non-organic chroma transmuters featuring significant thermic consistency as well as translucency, including phosphor-within-glass (PWG), are examined in the form of encasers applied to high-powered LED. The study herein concerns the influence from disparate phosphor forms featuring different chromas (LuAG, silicate, CASN as well as oxynitride) upon the dependability as well as degeneration for separate PWG encasers in the case of high-powered LED apparatuses. Regarding said goal, one glass constitution was individually blended into every phosphor form before undergoing a sintering process under proper heat levels, creating respective PWGs. The dependability in said PWGs underwent examination via conventional quickened aging experiments. Brightness penalties as well as variances for chroma coordinate results from the PWGs underwent assessment prior as well as posterior to aging. Thermic as well as dampness-generated abatement mechanism underwent assessment as well. The exterior for PWGs with disparate phosphor samples degenerated disparately, likely caused by formational inconsistencies among the glass latticework as well as phosphor form. As such, identifying the consistency for the glass constitution alongside the employed phosphor form proves paramount for guaranteeing prolonged consistencies for encasers applied to LED apparatuses in the market.

Keywords

$Ca_{14}Mg_2(SiO_4)_8$: Eu^{2+}, High Luminous Flux, Color Quality, Green-Emitting Phosphor, White Light Emitting Diodes

Received: 12 December 2025, Accepted: 31 March 2026
https://doi.org/10.26554/ijmr.20264281

1. INTRODUCTION

Light-emitting diode (LED) technology has progressively replaced conventional lighting systems owing to its high luminous efficacy, long operational lifetime, low energy consumption, and environmental safety (Luo et al., 2020; That et al., 2020). Continuous improvements in phosphor materials, semiconductor chips, and packaging architectures have significantly enhanced the photometric performance of white LED systems (Tran et al., 2020a; Thi et al., 2020d). Despite these advances, long-term reliability remains a critical concern, particularly in phosphor-converted white LEDs (pc-LEDs), where optical and thermal stresses directly influence device stability (Tran et al., 2020c; Zhang et al., 2020).

In pc-LED systems, blue or ultraviolet emissions from the semiconductor chip are partially converted into longer-wavelength radiation (yellow, green, or red) (Zhang et al., 2020) through photoluminescent phosphor layers. The overall luminous efficiency and chromatic stability of the device strongly depend on the conversion efficiency, chemical stability, and thermal robustness of the phosphor materials (Cong et al., 2025; Phuong Loan and Quoc Anh, 2020b). Although numerous phosphor compositions have been developed for solid-state lighting, only a limited number exhibit sufficient compatibility with LED operation conditions (Loan and Anh, 2020b; Trang and Anh, 2025). Common challenges include limited conversion efficiency, reabsorption losses, morphological irregularities, thermal quenching, and moisture-induced degradation, all of which can compromise practical deployment (Anh et al., 2025a,b).

Phosphor degradation is primarily driven by thermal stress, chemical instability, and prolonged optical irradiation. When degradation surpasses acceptable limits, luminous output decreases, spectral distribution shifts, and device lifetime shortens significantly. For example, alkaline earth sulfide and thiogallate phosphors exhibit strong emission intensity and desirable chromatic properties but are highly sensitive to humidity (Loan et al., 2025; Le et al., 2026). Meanwhile, alkaline earth orthosilicate phosphors offer moderate efficiency and suitable emission characteristics for lighting applications (Su and Gao, 2020), yet they also experience rapid deterioration under humid, high-

temperature, or continuous irradiation conditions. These limitations highlight the necessity of systematically understanding moisture-related degradation mechanisms at phosphor surfaces to enhance material stability and improve long-term LED reliability (Anh, 2020; Phuong Loan and Quoc Anh, 2020a; Thi et al., 2020a).

To mitigate environmental and thermal stress, remote phosphor configurations have been introduced, in which phosphor materials are embedded within glass matrices to provide mechanical and chemical protection (Loan and Anh, 2020b; Thi et al., 2020b). Although this approach improves thermal distribution and optical uniformity, degradation phenomena may still occur within both phosphor particles and the surrounding glass network when exposed to moisture or elevated temperatures. Furthermore, the fabrication of phosphor–glass composites (PWGs) requires careful control of glass transition and sintering temperatures to prevent phosphor decomposition or undesirable interfacial reactions (Tran et al., 2020b; Chen et al., 2020). Alkali modifiers are often introduced to lower glass transition temperatures; however, excessive alkali incorporation can destabilize the glass structure and adversely affect phosphor performance (Le et al., 2025; Loan and Anh, 2020b).

Despite extensive research on phosphor compositions, degradation behavior, and remote phosphor structures, existing studies predominantly focus on material synthesis, optical characterization, or short-term stability evaluation (Le et al., 2021). A systematic investigation that correlates moisture exposure conditions with surface degradation mechanisms in both phosphor particles and phosphor–glass composites remains limited. In particular, the interaction between humidity, glass matrix composition, and phosphor stability has not been comprehensively clarified under controlled environmental conditions (Thi et al., 2020d). This lack of integrated understanding restricts the development of optimized phosphor–glass systems for long-term solid-state lighting applications.

While previous studies have focused on phosphor synthesis or short-term stability, a significant research gap remains regarding the synergistic interaction between moisture exposure and surface degradation. This study adopts a systematic approach by concurrently evaluating the impact of hygrothermal stress on both pristine phosphor powders and phosphor-within-glass (PWG) structures. The core novelty lies in establishing a direct correlation between the glass matrix, the chemical nature of diverse phosphors (LuAG, silicate, CASN, and oxynitride), and the resulting degradation mechanisms. This provides a comprehensive framework for selecting materials to enhance the long-term reliability of high-power LED devices (Loan et al., 2025; Nguyen and Nguyen, 2025).

2. EXPERIMENTAL SECTION

2.1 Materials and Synthesizing Procedure

The experimental methodology was designed to systematically evaluate the compatibility between glass matrices and different phosphor systems, with the objective of optimizing thermal stability, optical performance, and environmental durability of phosphor-in-glass (PWG) structures. The glass matrix was formulated from pure H_3BO_3, SiO_2, ZnO, and Na_2CO_3, acquired from Sigma-Aldrich to provide a balance between low softening temperature, adequate chemical durability, and optical transparency in the visible region. The powdered raw materials were homogeneously mixed within one hour using a tubular oscillation blender (model T2F, Glen Mills Inc., USA) to minimize compositional inhomogeneity and ensure reproducible melting behavior apparatuses (Anh et al., 2025a; Le et al., 2025). The mixture was melted in an aluminum crucible for one hour under 1200 °C to guarantee complete liquefaction and phase homogenization (Loan and Anh, 2020a), forming bulk glass cullets. The melt was cast onto a flat metal plate and cooled naturally in air to avoid rapid quenching-induced stress. The resulting cullets were ball-ground for approximately ten minutes to produce glass frits via one planetary mono milling apparatus (Pulverisette-7, Fritsch, Germany) with controlled particle size, ensuring uniform phosphor dispersion during subsequent mixing (Anh, 2020; Phuong Loan and Quoc Anh, 2020a; Thi et al., 2020c).

A hot-stage microscope (Misura HSM, Expert System Solutions, Inc., Italy) was used to determine the glass softening temperature of 580oC for the powdered glass and thermal deformation range of the prepared glass frits, since the sintering temperature must remain below phosphor degradation thresholds while enabling sufficient viscous flow for densification. 10 vol% of four representative phosphor systems, LuAG ($Lu_3Al_5O_{12}$:Ce^{3+}), silicate (Sr_2SiO_4:Eu^{2+}), CASN ($CaAlSiN_3$:Eu^{2+}), and oxynitride ($(Sr,Ba)Si_2O_2N_2$:Eu^{2+}) (FORCE4 Co. Ltd., Korea), were incorporated at an identical glass weight fraction (90%) to enable objective comparison of interfacial compatibility and emission stability. The phosphor–glass mixtures were blended for one hour using a rotational mixer to ensure uniform particle distribution and minimize agglomeration (Tung et al., 2024). The powders were then compressed into pellets via a cast with a diametric magnitude of 32 mm for aridity strain test as well as a 12-mm counterpart for thermic abatement test. The compressed compounds underwent a sintering process under 580 °C within half an hour inside a furnace with a firing pace reaching 10oC per minute, a duration selected to allow viscous consolidation without excessive crystallization of the glass phase. The PWG discs were ground and polished to a breadth reaching 500 μm to obtain optically smooth surfaces for reliable photometric measurement (Loan et al., 2022; Luo et al., 2020; Tran et al., 2020c).

2.2 Instrument and Characterization

The optical as well as chemical stability for the PWGs under an aging process at 85 °C/85% RH were assessed posterior to 250, 500, 750, as well as 1000 hours. Prior to device-level testing, the PWGs underwent comprehensive optical characterization to correlate structural integrity with emission performance. Chromaticity coordinates and luminous flux were measured using an integrating sphere (GS-1290-LED spectrometer, GAMMA SCIENTIFIC, USA) to eliminate angular bias and ensure quantitative comparability. The characterization data of the PWGs can be seen in Figure 1. To assess microstructural integrity, phase stability, and potential

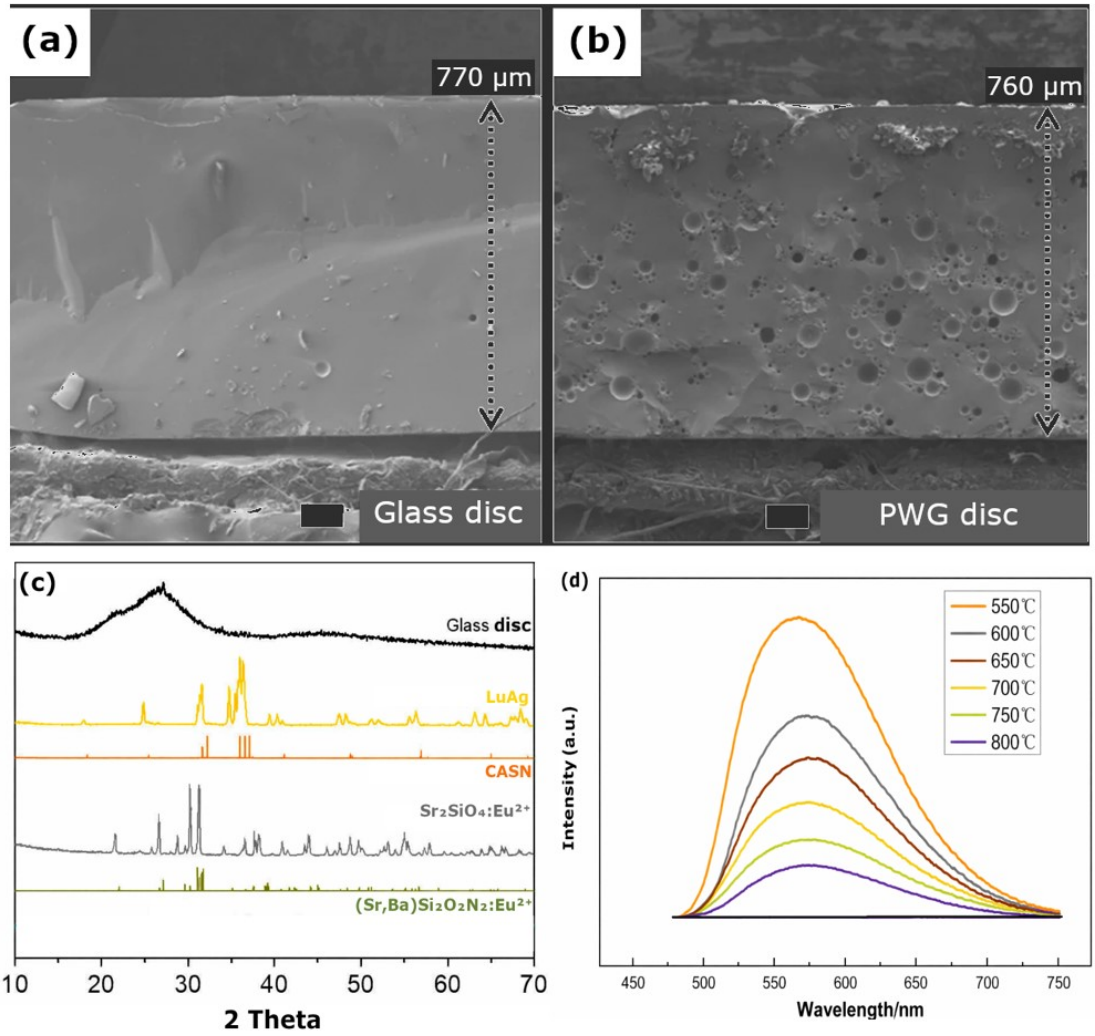

Figure 1. Characterization Data of PWG: (a) SEM Visual of Glass Disc, (b) SEM Visual of PWG Disc (c) XRD Patterns, (d) PL Spectra

glass–phosphor reactions, SEM analysis was conducted by scanning electronic microscopic assessment (S-4200, Hitachi, Japan), as seen in Figures 1(a) and (b), and XRD analysis was conducted by X-ray diffractometric assessment (X'Pert, Pro MRD, Phillips, Netherland), as seen in Figure 1(c). Photoluminescence (PL) spectra were obtained via one fluorescent spectrometric apparatus (F-4500 FL, Hitachi, Japan) to evaluate spectral shifts, emission intensity, and bandwidth stability under thermal treatment, as seen in Figure 1(d).

To further assess robustness under environmental stress, both phosphor powders and glass frits were subjected to controlled water immersion followed by a firing cycle at 75 °C (75 °C/100% RH) within 200 hours. This procedure was designed to simulate moisture-assisted chemical alteration during long-term operation (Nguyen and Nguyen, 2025). After drying in an oven for 24 hours under 65 °C, treated and untreated samples were comparatively analyzed in terms of microstructure, phase stability, and optical output. The PWGs accompanied by the phosphor samples, LuAg, silicate, CASN, as well as oxynitride, underwent exposure to 85 °C/85% RH within 1000 hours. The optical attributes as well as chemical alterations upon the exteriors of the PWGs, and upon the exteriors of the powdered phosphor as well as glass frits under exposure to 75 °C/100% RH within 200 hours were assessed. This comparative framework enabled evaluation of chemical durability, hydrolysis resistance, and structural resilience of the PWG system under realistic environmental conditions.

3. RESULTS AND DISCUSSION

The degeneration for the optical attributes in the PWGs would be caused by the degeneration of the exteriors for the phosphor as well as glass lattice. Figure 1(a) and (b) displays the exterior of a sintered glass disc and PWG disc and exhibits the buildup of crystalline granules or hydrates upon certain portions of its exterior posterior to the 85 °C/85% RH within 1000-hour testing. The crystal granules or hydrates comprise Zn, potentially ZnO or $Zn(OH)_2$, as well as certain sodium or silicon hydrates which

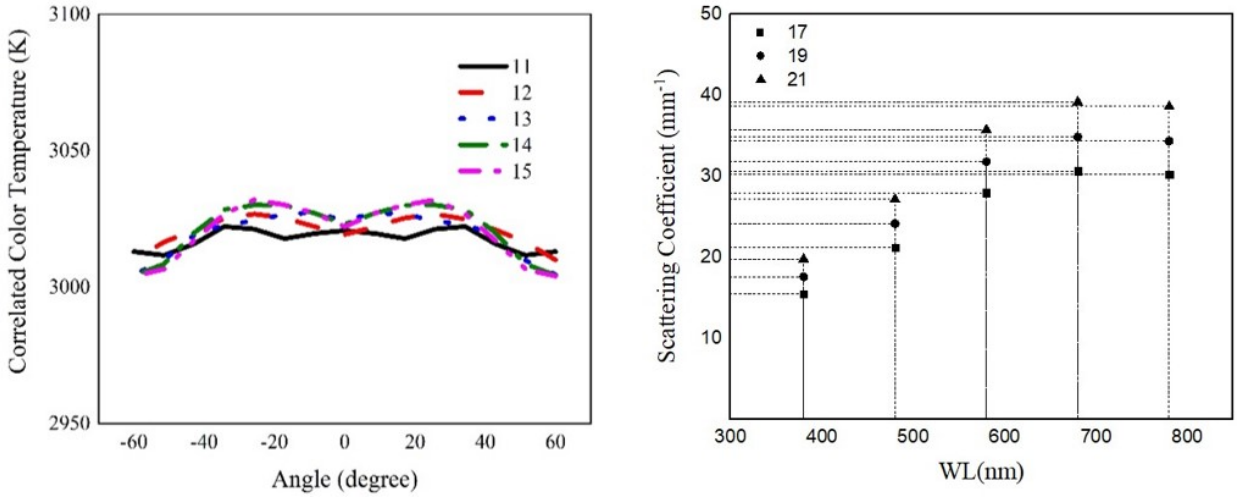

Figure 2. Relationship Between Scattering Coefficient and Wavelength

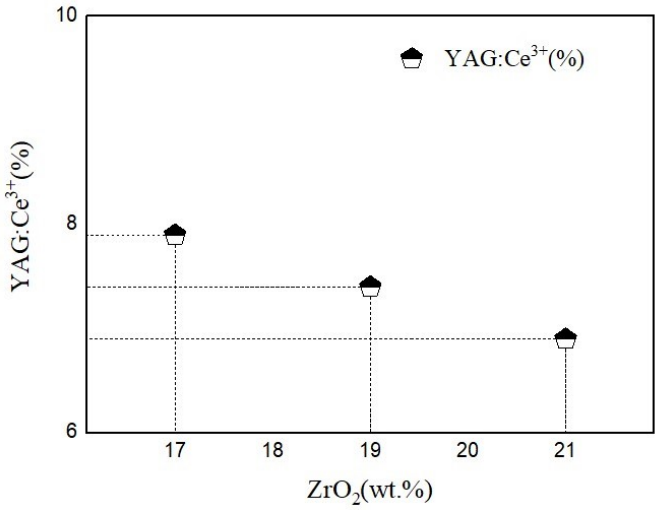

Figure 3. YAG:Ce Presence Interacting with Particle Size of SiO_2

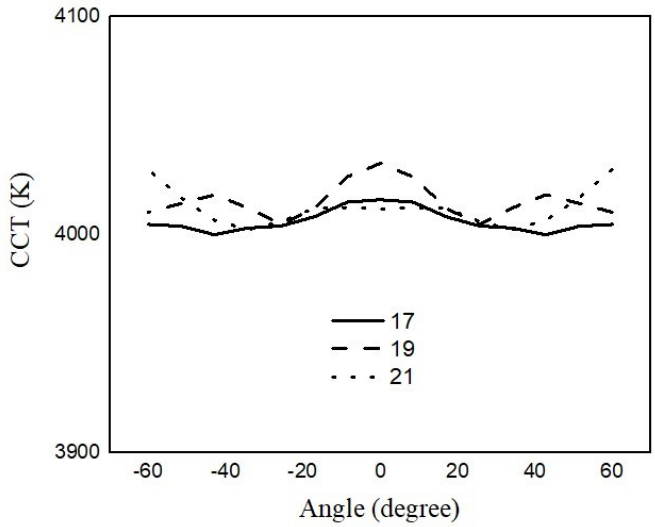

Figure 4. CCT Alteration Based on Particle Size

presumably manifested (Thi et al., 2020a, 2021).

Throughout exposure, the exterior of every PWGs would become coarse posterior to 200 hours as well as 1000 hours under 85 °C/85% RH. The silicate phosphor was not properly connected with the glass frit exterior even prior to processing, resulting from the disparity for the thermic extension coefficients for the glass as well as silicate phosphor. Under surging time within the 85 °C/85% RH condition, the silicate phosphor would be separated from the glass exterior then is subject corrosion. Certain forms of crystal granules or hydrates manifested upon certain parts of the exteriors of the PWGs featuring LuAg as well as oxynitride phosphor samples. However, they were only partially enveloped by hydrates posterior to the exposure duration. If not, the optical attributes of the LED will be subject to more degeneration.

The hydrates or crystal granules upon the PWGs featuring LuAg as well as oxynitride were assessed via XRD. The exteriors for said PWGs started crystallizing posterior to being exposed within 1000 hours but only showed incomplete crystallization. Notably, the crystal granules or hydrates comprised Zn, potentially ZnO or $Zn(OH)_2$, and an amount of sodium or silicon hydrates manifested as well, as seen in Figure 1(c). Since the manifested sheet proved sparse, there is a high possibility that the LuAg apexes manifested within the XRD spectra via the exterior beneath said sheet.

The PL intenseness for every unprocessed PWGs as well as PWGs posterior to being exposed within 1000 hours under 85 °C/85% RH was assessed in association with heat level. The PL intenseness for the PWGs under exposure decline under heat level at a greater degree than the counterpart of the matching

PWGs prior to being exposed. As seen in Figure 1(d), every PWG under exposure to aridity displayed higher thermic luminescent abatement, surpassing the matching unprocessed counterpart. The trigger power, Ea, regarding thermic abatement will be determined via:

$$\ln\left(\frac{l_0}{l}\right) = \ln A - \frac{E_a}{KT} \quad (1)$$

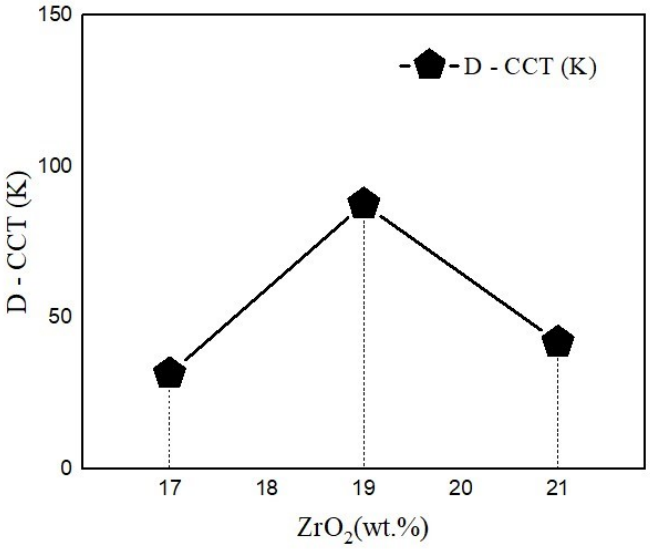

Figure 5. Variation in Hue Aberration Under SiO_2 Particle Size

in which I_0 and I respectively signify the luminescent intenseness for the PWG under room temperature and the operation temperature. A signifies a constant. K signifies the Boltzmann constant. The trigger powers for unprocessed PWGs featuring LuAg, silicate, CASN, and oxynitride phosphor samples were respectively computed to be 0.306, 0.407, 0.16, and 0.257 eV. The trigger powers posterior to processing within 1000 hours for said PWGs respectively reached 0.224, 0.194, 0.15, and 0.155 eV.

The degradation of glass lattice structures and phosphor materials has a pronounced impact on the emission intensity of LED devices. In phosphor-converted LED systems, white light is generated through the combined contribution of residual blue emission from the diode and wavelength-converted yellow emission from the phosphor embedded within or coated on the phosphor–window glass (PWG). The final luminous output therefore depends on the optical balance between blue transmission, phosphor absorption, and re-emission efficiency.

When the surfaces of the glass lattice or phosphor layer become roughened, eroded, or chemically altered due to prolonged thermal or optical stress, the propagation of blue photons through the PWG is significantly modified. Increased surface roughness enhances diffuse scattering, reducing the fraction of blue photons that effectively reach and excite the phosphor. Instead of contributing to radiative conversion, a larger portion of the incident blue light is scattered or lost, leading to a reduction in total emission intensity. From a theoretical perspective, this behavior aligns with scattering theory in particulate media, where changes in particle size or surface morphology alter the scattering cross-section and angular redistribution of light.

In addition to physical degradation, oxidation of the phosphor activator ions further exacerbates emission loss. Once the activator undergoes oxidation, it may absorb incident photons without contributing to radiative recombination, instead dissipating energy via nonradiative relaxation pathways. This reduces effective quantum efficiency while increasing localized heat generation, which in turn accelerates further structural degradation. Consequently, both the host lattice and the activator ions govern the balance between absorption, scattering, and emission processes. Their structural and chemical stability is therefore essential for maintaining high luminous output and long operational lifetimes in LED devices.

The optical characteristics of PWGs operating with blue diode units were evaluated before and after exposure under different durations and humidity conditions. Lumen depreciation and chromatic coordinate shifts were clearly observed after exposure. PWGs incorporating silicate-based phosphor compositions exhibited the most severe degradation, showing larger lumen penalties and greater chromatic drift. CASN-based PWGs also experienced degradation, although with improved stability compared to silicate systems. In contrast, PWGs containing oxynitride and LuAG phosphors demonstrated minimal lumen loss and smaller chromatic deviations, indicating superior resistance to environmental stress. Surface inspection revealed that prolonged exposure promotes crystal or hydroxide formation on PWG surfaces, eventually blocking photon transmission and reducing optical usability. These findings reinforce the mechanism that surface chemical reactions directly disrupt photon transport and conversion efficiency.

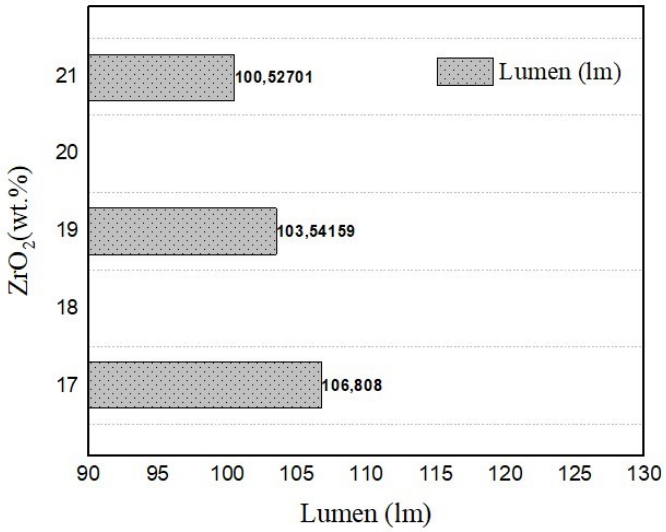

Figure 6. LED Lumen Generated Based on SiO_2 Particle Size

Figure 2 illustrates the wavelength dependence of the scattering coefficient. The general increase in scattering with wavelength promotes angular redistribution of blue-chip emission and enhances interaction probability within the phosphor layer, thereby facilitating wavelength conversion. However, a noticeable reduction in scattering near 800 nm suggests a wavelength-dependent scattering efficiency likely associated with refractive index contrast. When forward blue-light dispersion dominates while repetitive absorption and backward scattering are suppressed, luminescence enhancement is observed. This balance reflects the theoretical competition between scattering-assisted excitation and scattering-induced optical loss.

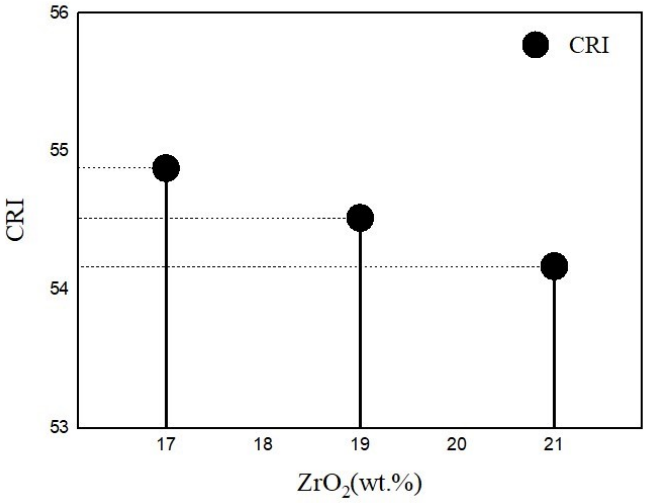

Figure 7. CRI Values with Various SiO_2 Proportions

Figure 3 shows that as SiO_2 particle size increases, the YAG:Ce phosphor content must be reduced to maintain spectral balance. Larger particles exhibit stronger scattering cross-sections, meaning less phosphor concentration is required to achieve similar color conversion. This inverse relationship supports the theoretical expectation that scattering strength scales with particle dimension.

The influence of particle size on correlated color temperature (CCT) is presented in Figure 4. Pronounced CCT fluctuations occur around 17–19 wt.%, where the system becomes highly sensitive to the balance between blue leakage and yellow conversion. For non-specialist readers, CCT reflects the "warm" or "cool" appearance of white light. When scattering increases excessively, the spectral balance shifts toward longer wavelengths, producing measurable CCT variation. The minimum CCT observed at 17 wt.% and maximum at 19 wt.% indicate a narrow optimization window where scattering and conversion reach dynamic equilibrium.

Figure 5 demonstrates that chromatic aberration varies significantly with particle size. A sharp increase in hue deviation at 19 wt.% indicates instability in spectral mixing due to excessive scattering. Beyond this region, aberration decreases as backward redistribution stabilizes the emission balance. These variations highlight the delicate interplay between scattering strength and color uniformity. In contrast, Figure 6 shows that luminous flux decreases steadily as particle size increases. Enhanced backward scattering and repeated absorption processes reduce forward light extraction efficiency. Larger particle sizes effectively lengthen the optical path within the phosphor layer, increasing reabsorption probability and lowering total spectral energy output. This trend is consistent with radiative transport principles in diffusive media.

The color rendering performance shown in Figures 7 and 8 indicates slight decreases in CRI and CQS with increasing particle size. Excessive scattering favors orange–yellow emission over balanced blue and green components, resulting in minor color distortion. CRI evaluates eight color samples, whereas CQS assesses fifteen and incorporates perceptual weighting. For broader accessibility, CRI represents how naturally colors appear under a given light source; reductions in CRI or CQS suggest minor deviations from ideal color reproduction. Thus, while increased scattering enhances wavelength conversion, it may compromise color fidelity when not carefully optimized.

To integrate the above observations, a comprehensive degradation pathway can be proposed. Under hygrothermal stress, moisture molecules diffuse into the PWG surface and preferentially react with susceptible components of the glass network or phosphor host lattice. This interaction promotes hydroxide formation and partial lattice disruption, leading to surface roughening and the development of microstructural defects. The increased surface irregularity modifies the effective refractive index contrast between glass and phosphor particles, thereby altering the scattering cross-section and angular distribution of incident blue photons. As scattering becomes stronger and less directionally controlled, a larger fraction of blue light undergoes backward redistribution or multiple internal reflections instead of contributing to forward radiative conversion. Simultaneously, chemical alteration of activator ions may introduce nonradiative recombination centers, reducing internal quantum efficiency. The combined effects of enhanced backscattering, repeated absorption, and nonradiative relaxation ultimately manifest as lumen depreciation and chromatic coordinate shift.

This mechanistic framework explains the hierarchy of stability observed among different phosphor systems. Silicate-based PWGs exhibit more pronounced hydroxide formation and structural vulnerability, leading to severe optical degradation. In contrast, oxynitride and LuAG phosphors demonstrate stronger lattice rigidity and lower susceptibility to moisture-induced disruption, thereby maintaining more stable photon transport and emission balance. Therefore, long-term reliability is governed not only by intrinsic phosphor efficiency but also by interfacial chemical compatibility and resistance to moisture-assisted structural evolution. Collectively, the trends presented in Figures 1–7 consistently support this mechanism by linking variations in scattering behavior to measurable changes in CCT, luminous flux, CRI, and CQS. These correlations confirm that optical degradation is a multi-factorial phenomenon governed by both mi-

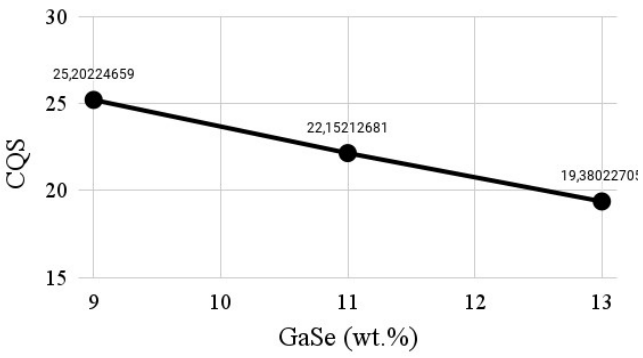

Figure 8. CQS Values with Various SiO_2 Proportions

crostructural evolution and radiative transport dynamics.

The results highlight a fundamental trade-off between scattering-enhanced conversion efficiency and luminous extraction performance. Optimized particle size enables controlled spectral tuning, allowing designers to adjust CCT for specific applications such as architectural lighting, display backlighting, and human-centric lighting systems where color temperature influences visual comfort and circadian response. Understanding degradation mechanisms also provides guidance for material selection in high-humidity or high-temperature environments. Oxynitride- and LuAG-based PWGs demonstrate superior environmental stability, making them promising candidates for outdoor, automotive, and high-power lighting systems. Future research may focus on surface passivation strategies to suppress hydroxide formation, advanced particle engineering to control scattering distributions, and numerical optical modeling to simulate photon transport within multilayer LED packages. Integrating experimental data with Monte Carlo simulations or radiative transfer models would further strengthen predictive design capabilities for next-generation phosphor-converted LED systems.

4. CONCLUSIONS

In conclusion, this research demonstrates that the degradation of the glass matrix and phosphor surfaces is the primary driver of luminous decay in high-power LEDs. Our findings reveal a clear hierarchy of stability: Silicate phosphors exhibited the most severe degradation due to surface hydroxide formation, while Oxynitride and LuAG phosphors maintained the most stable optical performance. The observed lumen penalty is attributed to enhanced backscattering and re-absorption caused by surface chemical modifications. These results confirm that optimizing the compatibility between the glass host and phosphor type is essential for the operational reliability of remote-phosphor systems in outdoor and automotive lighting applications.

5. ACKNOWLEDGEMENT

The authors wish to express their gratitude to the Posts and Telecommunications Institute of Technology, Vietnam, for financial support for this research.

REFERENCES

Anh, N. (2020). The Application of Green YF_3: Er^{3+}, Yb^{3+} and Red $MgSr_3Si_2O_8$: Eu^{2+}, Mn^{2+} Layers to Remote Phosphor LED. *TELKOMNIKA (Telecommunication Computing Electronics and Control)*, **18**(6); 3234–3239

Anh, N. D. Q., S. D. Ho, P. T. M. Man, T. K. Duy, and N. T. P. Loan (2025a). Obtaining Higher LED's Lighting Chromaticity And Luminosity With SiO_2 Particles At Different Diameters. *Journal of Advanced Engineering and Computation*, **9**(1); 21–28

Anh, N. D. Q., N. T. P. Loan, P. Van De, and H. Lee (2025b). Potassium Bromide Scattering Simulation For Improving Phosphor-Converting White LED Performance. *Optoelectronics and Advanced Materials: Rapid Communications*, **19**(7–8); 378–383

Chen, M. J., N. T. P. Loan, L. V. Tho, T. M. Bui, P. X. Le, N. D. Q. Anh, H. Y. Liao, J. C. Chang, and H. Y. Lee (2020). The Impacts Of $Ba_2Li_2Si_2O_7$:Sn^{2+}, Mn^{2+} And $CaMgSi_2O_6$:Eu^{2+}, Mn^{2+} Particles On The Optical Properties Of Remote Phosphor LED. *Materials Science-Poland*, **38**(1); 197–205

Cong, P. H., N. T. P. Loan, N. D. Q. Anh, and H.-Y. Lee (2025). Influence Of Potassium Bromide Phosphor On Optical Properties Of White Light-Emitting Diodes. *International Journal of Advances in Applied Sciences*, **14**(4); 1359–1366

Le, P. X., S. D. Ho, N. D. Quoc Anh, and H.-Y. Lee (2021). Triple-Layer Remote Phosphor Structure: A Potential Packaging Configuration To Enhance Both Color Quality And Lumen Efficiency Of 6,000–8,500 K WLEDs. *Materials Science-Poland*, **39**(4); 458–466

Le, P. X., N. T. P. Loan, and N. D. Q. Anh (2026). Optical Assessment Of TiO_2 Employed In Phosphor-Transmuted WLED Devices. *Science and Technology Indonesia*, **11**(1); 345–355

Le, P. X., N. T. P. Loan, N. D. Q. Anh, and H.-Y. Lee (2025). Thermally Stable Sol-Gel Yttrium Aluminum Garnet Cerium Phosphors For White Light-Emitting Diodes. *International Journal of Advances in Applied Sciences*, **14**(4); 1367–1374

Loan, N. T. P. and N. D. Q. Anh (2020a). $Na_3Ce(PO_4)_2$:Tb^{3+} and $Na(Mg_{2-x}Mn_x)LiSi_4O_{10}F_2$:Mn Phosphors: A Suitable Selection For Enhancing Color Quality And Luminous Flux Of Remote White Light-Emitting Diodes. *TELKOMNIKA (Telecommunication Computing Electronics and Control)*, **18**(4); 2095–2100

Loan, N. T. P. and N. D. Q. Anh (2020b). The Effects of ZnO Particles on the Color Homogeneity of Phosphor-Converted Highpower White LED Light Sources. *International Journal of Electrical and Computer Engineering (IJECE)*, **10**(5); 5155–5161

Loan, N. T. P., N. D. Q. Anh, P. T. M. Man, and H.-Y. Lee (2025). Assessing Thermic Degradation For Yttrium-Aluminum Precursive Agents Applied To YAG Phosphor Samples. *Science and Technology Indonesia*, **10**(4); 1209–1214

Loan, N. T. P., N. D. Q. Anh, N. C. Trang, and H.-Y. Lee (2022). Better Color Distribution Uniformity And Higher Luminous

Intensity For LED By Using A Three-Layered Remote Phosphor Structure. *Materials Science-Poland*, **40**(1); 60–67

Luo, G.-F., N. T. P. Loan, L. Van Tho, N. D. Q. Anh, and H.-Y. Lee (2020). Enhancement Of Color Quality And Luminous Flux For Remote-Phosphor LEDs With Red-Emitting $CaMgSi_2O_6:Eu^{2+}$, Mn^{2+}. *Materials Science-Poland*, **38**(3); 409–415

Nguyen, V. D. and D. Q. A. Nguyen (2025). $Ba_3GdNa(PO_4)_3F:Eu^{2+}$ Phosphor With Blue-Red Emission Colors On White-LED Properties. *International Journal of Electrical and Computer Engineering Systems*, **38**(3); 1564–1571

Phuong Loan, N. T. and N. D. Quoc Anh (2020a). The Application Of Double-Layer Remote Phosphor Structures In Increasing WLEDs Color Rendering Index And Lumen Output. *International Journal of Electrical and Computer Engineering (IJECE)*, **10**(5); 5183–5190

Phuong Loan, N. T. and N. D. Quoc Anh (2020b). Improving Color Quality And Luminous Flux Of White LED Utilizing Triple-Layer Remote Phosphor Structure. *International Journal of Electrical and Computer Engineering (IJECE)*, **10**(5); 5168–5174

Su, V.-C. and C.-C. Gao (2020). Remote GaN Metalens Applied To White Light-Emitting Diodes. *Optics Express*, **28**(26); 38883–38891

That, P. T., T. M. Bui, N. T. P. Loan, P. X. Le, N. D. Q. Anh, and L. V. Tho (2020). Dual-Layer Remote Phosphor Structure: A Novel Technique To Enhance The Color Quality Scale And Luminous Flux Of WLEDs. *International Journal of Electrical and Computer Engineering (IJECE)*, **10**(4); 4015–4022

Thi, M. H. N., T. M. Bui, and N. D. Q. Anh (2021). Aiming To The Superior Of Phosphor Pattern: Influence Of SiO_2 Nanoparticles On Photoluminescence Intensification Of YAG:Ce. *International Journal of Electrical and Computer Engineering (IJECE)*, **11**(6); 4833–4839

Thi, M. H. N., N. T. P. Loan, and N. D. Q. Anh (2020a). Acquiring Higher Lumen Efficacy And Color Rendering Index with Green $NaYF_4:Er^{3+}$, Yb^{3+} and Red α-$Sr_{O.3}B_2O_3:Sm^{2+}$ Layers For Designing Remote Phosphor LED. *TELKOMNIKA (Telecommunication Computing Electronics and Control)*, **18**(6); 3222–3228

Thi, M. H. N., N. T. P. Loan, and N. D. Q. Anh (2020b). Study Of Red-Emitting $LaAsO_4:Eu^{3+}$ Phosphor For Color Rendering Index Improvement Of WLEDs With Dual-Layer Remote Phosphor Geometry. *TELKOMNIKA (Telecommunication Computing Electronics and Control)*, **18**(6); 3210–3215

Thi, M. H. N., P. T. That, and N. D. Q. Anh (2020c). Eu^{2+} Activated Strontium-Barium Silicate: A Positive Solution for Improving Luminous Efficacy and Color Uniformity of White Light-Emitting Diodes. *Materials Science-Poland*, **38**(4); 594–600

Thi, M. H. N., P. T. That, N. D. Q. Anh, and T. Thanh (2020d). Triple-Layer Remote Phosphor Structure: A Novel Option for the Enhancement of WLEDs' Color Quality and Luminous Flux. *Materials Science-Poland*, **38**(4); 654–660

Tran, A.-M. D., N. D. Q. Anh, and N. T. P. Loan (2020a). Enhancing Light Sources Color Homogeneity in High-Power Phosphor-Based White LED Using ZnO Particles. *Telecommunication Computing Electronics and Control*, **18**(5); 2628–2634

Tran, A.-M. D., N. D. Q. Anh, and N. T. P. Loan (2020b). The Influences of Calcium Fluoride and Silica Particles on Improving Color Homogeneity of WLEDs. *Telecommunication Computing Electronics and Control*, **18**(5); 2696–2701

Tran, T. C., N. D. Q. Anh, and N. T. P. Loan (2020c). Comparison of Calcium Carbonate and Titania Particles on Improving Color Homogeneity and Luminous Flux of WLEDs. *TELKOMNIKA (Telecommunication Computing Electronics and Control)*, **18**(5); 2690–2695

Trang, L. T. and N. D. Q. Anh (2025). Influences From SiO_2 Particles On Optical Properties Of White Diodes Verified Through Computer Simulation. *Indonesian Journal of Electrical Engineering and Computer Science*, **38**(3); 1572–1579

Tung, H., B. Minh, N. Thai, H. Lee, and N. Anh (2024). ZnO Particles As Scattering Centers to Optimize Color Production and Lumen Efficiencies of Warm White LEDs. *Optoelectronics and Advanced Materials-Rapid Communications*, **18**; 283–288

Zhang, T., X. Zhang, B. Ding, J. Shen, Y. Hu, and H. Gu (2020). Homo-Epitaxial Secondary Growth Of ZnO Nanowire Arrays For A UV-Free Warm White Light-Emitting Diode Application. *Applied Optics*, **59**(8); 2498–2505

